Intercellular Receptor-ligand Binding: Effect of Protein-membrane Interaction

Long Li [1,2], **Jing Ji** [3*], **Fan Song** [2,4] and **Jinglei Hu** [1*]

1 - *Kuang Yaming Honors School and Institute for Brain Sciences,* Nanjing University, 210023 Nanjing, China
2 - *State Key Laboratory of Nonlinear Mechanics and Beijing Key Laboratory of Engineered Construction and Mechanobiology,* Institute of Mechanics, Chinese Academy of Sciences, 100190 Beijing, China
3 - *Key Laboratory of Biomechanics and Mechanobiology (Beihang University),* Ministry of Education Beijing Advanced Innovation Center for Biomedical Engineering School of Biological Science and Medical Engineering, Beihang University, Beijing 100083, China
4 - *School of Engineering Science,* University of Chinese Academy of Sciences, 100049 Beijing, China

Correspondence to Jing Ji and Jinglei Hu: 09714@buaa.edu.cn (J. Ji), hujinglei@nju.edu.cn (J. Hu)
https://doi.org/10.1016/j.jmb.2022.167787
Edited by Dechang Li

Abstract

Gaining insights into the intercellular receptor-ligand binding is of great importance for understanding numerous physiological and pathological processes, and stimulating new strategies in drug design and discovery. In contrast to the *in vitro* protein interaction in solution, the anchored receptor and ligand molecules interact with membrane *in situ*, which affects the intercellular receptor-ligand binding. Here, we review theoretical, simulation and experimental works regarding the regulatory effects of protein-membrane interactions on intercellular receptor-ligand binding mainly from the following aspects: membrane fluctuations, membrane curvature, glycocalyx, and lipid raft. In addition, we discuss biomedical significances and possible research directions to advance the field and highlight the importance of understanding of coupling effects of these factors in pharmaceutical development.

Introduction

Cells communicate directly with one another *via* intercellular interactions of receptors and ligands anchored on apposing membranes to govern numerous biological processes, such as signal transduction, immune responses, tissue formation, as well as cancer invasion and metastasis.[1–8] The key properties quantifying the intercellular receptor-ligand interactions are on- and off-rate constants k_{on} and k_{off}, and binding affinity $K_a = k_{on} / k_{off}$. The binding affinity is also related to the densities of free receptors [R], free ligands [L], and receptor-ligand complexes [RL], i.e., $K_a = [RL] / ([R][L])$.[7,9] Investigation of intercellular receptor-ligand binding helps to understand the molecular mechanisms underlying cellular activities and is of fundamental significance to drug design and biomedical applications. For example, the binding kinetics of neuronal adhesion proteins, such as presynaptic neurexins and postsynaptic neuroligins, are shown to depend strongly on their molecular structures and play an essential role in transsynaptic adhesion and synapse formation.[10–17] It has been suggested that amyloid-β (Aβ) oligomers bind to neuroligin-1 with high affinity, impairing neurotransmission signaling mediated by neurexin-neuroligin transsynaptic interaction and leading to neurotoxicity and synaptic dysfunction. Therefore, intervention of the binding provides a promising therapeutic option for Alzheimer's disease.[18–19] In addition, the dynamic interactions between CD47

overexpressed on the surface of many types of cancer cells and signal-regulatory protein α (SIRPα) anchored on the macrophage regulate the phosphorylation of immunoreceptor tyrosine-based inhibitory motif (ITIM) in the cytoplasmic tail of SIRPα and the activation of phosphatases including SHP-1 and SHP-2, which enable the escape of the cancer cells from macrophage-mediated phagocytosis.[20–21] Anti-cancer therapy targeting the CD47-SIRPα binding affinity has been demonstrated to promote the adaptive immune response and enhance the phagocytosis of tumor cells by macrophages.[20,22–23] In view of these, studying on the intercellular receptor-ligand binding kinetics has been hotspots and frontiers in the field of chemistry, physics, biology and medicine.

Much of our early understanding of receptor-ligand binding kinetics comes from the *in vitro* three-dimensional (3D) measurement by surface plasmon resonance (SPR) for soluble variants of the receptors and ligands that lack the membrane anchors or transmembrane domains.[24] SPR studies on the interactions of T cell receptor (TCR) with different types of peptide-major histocompatibility complex (pMHC) have revealed that the functional outcome of T cell correlates closely with the TCR-pMHC binding kinetics.[25–26] Specifically, the average lifetime ($1 / k_{off}$) of TCR-pMHC complexes crucially determines the strength of T cell signaling and responsiveness.[27–28] SPR measurements have provided valuable information on the kinetics of receptor-ligand interactions. However, there are significant limitations in SPR measurements since the membrane environment that affects the binding is completely missing. A variety of experimental techniques have been developed to study *in situ* the intercellular receptor-ligand binding that occurs in two dimensional (2D) membrane environment, including fluorescence spectroscopy,[29–32] micropipette aspiration,[9,33–34] atomic force microscopy,[35–37] as well as flow chamber.[38–40] Substantial differences have been found between 3D and 2D binding kinetics. For example, 3D SPR experiments show that the TCR binds to pMHC with relatively slow off-rate and low binding affinity.[41–42] In contrast, the 2D data measured by micropipette adhesion frequency and thermal fluctuation assays show that the TCR-pMHC interactions are of high affinity, and the 2D off-rates are up to 8,300-fold faster than their 3D counterparts.[9,41] Moreover, the 2D binding affinity of the same receptors and ligands measured from fluorescence recovery method and mechanical methods can differ by several orders of magnitude.[17,43] The significant discrepancy between experimental results has motivated further investigations on how protein-membrane interactions affect the intercellular receptor-ligand binding.

Here, we review representative works regarding the regulatory role of protein-membrane interactions in intercellular receptor-ligand binding mainly from the following aspects: (1) membrane fluctuations, (2) membrane curvature, (3) glycocalyx, (4) lipid raft. These studies shed lights on the biophysical interactions on the membrane interfaces during cell adhesion, and provided guidelines and strategies for drug design and disease treatment. Further, we describe the biomedical significance of these regulatory factors, and discuss possible future research directions especially in the context of neuronal synapse.

Membrane Fluctuations

Under physiological conditions, the fluid membranes undergo thermal shape fluctuations stimulated by, e.g., Brownian motion of water.[44–47] Receptors and ligands that are anchored in apposing membranes can only bind when the local separation of the two membranes is within an appropriate range. Therefore, the receptor-ligand complexes restrict the local membrane separation and perturb the fluctuations of the membranes. This type of protein-membrane interaction leads to *cis*-attraction between receptor-ligand complexes and cooperative binding of cell adhesion molecules, confirmed by experimental, theoretical, and simulation studies.[43,48–51] The physical picture is that the formation of receptor-ligand complexes suppresses the membrane fluctuations, which in turn facilitates the formation of additional receptor-ligand complexes (Figure 1(a)).

Molecular dynamics (MD) simulations with a molecular model for lipid membranes and rodlike transmembrane[7] or lipid-anchored[53] adhesion proteins (Figure 1(b)) demonstrated that the binding affinity K_a depends on the nanoscale thermal roughness $\xi_\perp$ of the two adhering membranes. For large roughness, $K_a \propto 1/\xi_\perp$. The on-rate constant k_{on} was found to decrease with the roughness $\xi_\perp$, whereas the off-raft constant k_{off} increases with $\xi_\perp$. That is, the membrane undulations make the binding more difficult and the unbinding easier, consistent with the theoretical prediction by Krobath et al.[43] Both k_{on} and k_{off} contribute to the roughness dependence of binding affinity.[7] Xu et al. performed Monte Carlo (MC) simulations of membrane adhesion, where the membranes are modeled by discretized elastic surfaces and the rodlike adhesion proteins diffuse along the membrane surfaces and can rotate around the membrane anchor (Figure 1(c)).[52] The MC simulations illustrated that the binding affinity also depends on both the length and rotational flexibility of the adhesion molecules in addition to the membrane roughness, since these two factors dictate the rotational entropy loss of the receptor-ligand pair upon binding in the membrane interface.[52]

All the aforementioned theoretical and simulation studies have dealt with stiff adhesion molecules.[7,43,52–53] For real adhesion proteins, their molecular conformations will change during binding. Intuitively, proteins with conformational flexibil-
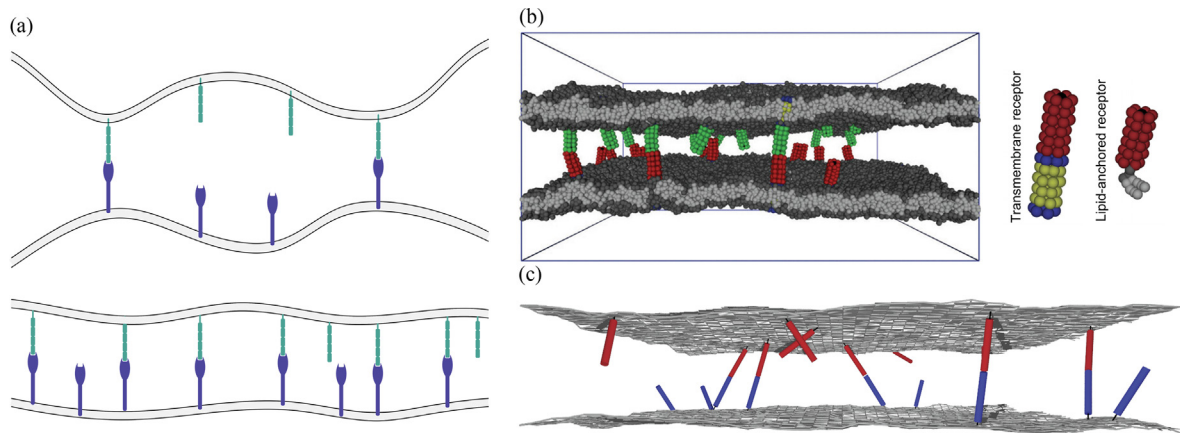
Figure 1. Membrane shape fluctuations are constrained by receptor-ligand complexes, leading to cooperative receptor-ligand binding. (a) The intercellular receptor-ligand binding depends sensitively on the membrane roughness caused by the thermally-excited shape fluctuations. The thermal membrane roughness decreases with increasing densities of binding proteins since receptor-ligand complexes suppress the membrane fluctuations, which in turn facilitates the formation of additional receptor-ligand complexes. (b) Snapshot from molecular dynamics simulations with a molecular model for lipid membranes and rodlike transmembrane or lipid-anchored proteins. (c) Snapshot from Monte Carlo simulations of two discretized elastic membranes with diffusing rodlike proteins that can rotate around the membrane anchor. Subfigures (b) and (c) are adapted from References,[7,52] respectively.

ity could adapt their conformations for binding in the membrane environment without strongly constraining the local membrane separation. A natural and important question then arises as to whether the membrane fluctuations affect the binding of real adhesion proteins. Steinkühler et al. experimentally investigated the CD47-SIRPα interaction that mediates the adhesion of cell-derived giant vesicles decorated with CD47 to SIRPα-functionalized substrate using fluorescent recovery after bleaching (FRAP).[29] They found that the binding affinity increases with the CD47-SIRPα complex concentration, verifying the membrane fluctuation-induced cooperative binding. This experiment undoubtedly demonstrated that membrane thermal undulations affect the binding of membrane-anchored receptors and ligands. However, it remains to be understood how the conformational flexibility of adhesion proteins is coupled with the membrane fluctuations and affect the binding kinetics. MD simulations with molecular models for (semi-)flexible adhesion proteins can provide valuable insights.

Now we review the theoretical approach to account for the binding affinity and rate constants of adhesion proteins affected by membrane fluctuations. The binding affinity K_a can be approximated as $K_a = \int K_a(l)P(l)dl$,[52–55] where $K_a(l)$ is the binding affinity of the binding pairs anchored to apposing planar membranes with separation l. The membrane profile $P(l)$ describes the distribution of local membrane separation l for membranes with thermally-excited shape fluctuations. This equation $K_a = \int K_a(l)P(l)dl$ indicates

that one can calculate K_a by simply averaging $K_a(l)$ over the probability distribution $P(l)$ for the local membrane separation l. $K_a(l)$ is determined by the free energy change of the receptor-ligand pair upon binding, and depends on properties of the receptor and ligand molecules such as conformational flexibility, overall length and rotational flexibility around the membrane anchor. In the case of two fluctuating membranes adhering *via* the binding of rodlike receptors and ligands, the membrane profile $P(l)$ follows approximately a Gaussian distribu-

tion $P(l) = \exp\left[-\left(l - \bar{l}\right)^2 / 2\xi_\perp^2\right] / \left(\sqrt{2\pi}\xi_\perp\right)$ with $\bar{l}$

is the average separation of the membranes, and

$\xi_\perp = \sqrt{\langle\left(l - \bar{l}\right)^2\rangle}$ is the relative roughness of the

two membranes and measures the strength of thermally excited membrane shape fluctuations.[7,53] Assuming a harmonic effective configurational energy for the receptor-ligand complex $H_{RL}(l) = \frac{1}{2}k_{RL}(l - l_0)^2$, one obtains $K_a(l) \propto \exp\left(-\frac{1}{2}k_{RL}(l - l_0)^2/k_B T\right)$ with l_0 being the preferred length of receptor-ligand complexes.[53] So the binding affinity $K_a \propto 1/\xi_\perp$ for large roughness $\xi_\perp$. As a length scale that characterizes the amplitude of the membrane fluctuations, the roughness $\xi_\perp$ is proportional to the average distance between neighboring receptor-ligand complexes that constrain the local separation of the membranes, i.e., $\xi_\perp \propto 1/\sqrt{[RL]}$. The binding of membrane-

anchored receptors and ligands then follows the law of mass action $[RL] = K_a[R][L] \propto [R]^2[L]^2$,[7] corresponding to the Hill coefficient of $n_H > 2$ as given by the slope of binding curves in the Hill plot of $\log([RL]/[R])$ versus $\log[L]$.[56] The equation $K_a = \int K_a(l)P(l)dl$ can also be applied to calculate the binding affinity of real adhesion proteins with molecular flexibility once $K_a(l)$ is measured.

The on-rate constant k_{on} generally depends on the diffusion of the molecules, the energy barrier for the formation of the receptor-ligand transition-state complex, and the dynamics of membrane shape fluctuations. In analogy to the equation $K_a = \int K_a(l)P(l)dl$, the on-rate constant k_{on} was approximated as $k_{on} = \int k_{on}(l)P(l)dl$,[52–55] where $k_{on}(l)$ is the on-rate constant of the binding pairs anchored to apposing planar membranes with separation l. This approximation is valid when the membrane fluctuations are much faster than the diffusion of the adhesion proteins on the relevant length scale for binding. The prediction of k_{on} by equation $k_{on} = \int k_{on}(l)P(l)dl$ agrees quantitatively with the measurement from MD simulations for rod-like adhesion proteins.[7,53] The on-rate constant was found to decrease with the thermal roughness of the two adhering membranes. The off-rate constant is then $k_{off} = k_{on}/K_a$. The theory for rodlike adhesion protein claims that at large roughness, $k_{on} \propto 1/\xi_\perp$, implying that $k_{on} \propto [R][L]$.[53] In contrast to stiff adhesion proteins, real proteins exhibit conformational fluctuations in addition to the lateral diffusion and rotation around the membrane anchor. How conformations of the adhesion proteins affect their binding kinetics remains to be investigated.

As mentioned in the Introduction section, the binding affinity measured from fluorescence recovery experiments and mechanical methods differs by several orders of magnitude.[17,43] In fluorescence recovery experiments, the binding affinity is measured in the equilibrium contact zone. In contrast, mechanical methods probe the binding affinity during initial contact having a smaller value of contact area. On the one hand, the average membrane separation in the fluorescence recovery method is close to the length of receptor-ligand complexes, thus facilitating the complex formation. The average separation in the mechanical methods is typically larger than the length of receptor-ligand complexes, which inhibits the receptor-ligand binding. On the other hand, compared to the case of initial contact in mechanical methods, the area concentration of receptor-ligand complexes $[RL]$ in the equilibrium contact zone for the fluorescence recovery method is larger due to the diffusion of free receptor and ligand.[32] The enhanced complex concentration reduces the relative membrane roughness and leads to larger values of binding affinity due to cooperative binding. The dependence of binding affinity on the average membrane separation and relative membrane roughness regulated by thermal membrane fluctuations helps to understand the orders-of-magnitude gap between the measured binding affinity by different methods.

Membrane Curvature

In addition to the thermal fluctuations, the shape of the membranes can also be perturbed by the binding proteins that are associated with cell membranes *via* transmembrane domains (e.g. integrins, cadherins) or glycosylphosphatidyl-inositol anchors (e.g. CD48). This perturbation can affect the binding of adhesion proteins. Mathematically, membrane shapes are characterized by two principal curvatures, c_1 and c_2 (or more commonly by two combinations of the principal curvatures, total curvature $c_1 + c_2$ and Gaussian curvature $c_1 \cdot c_2$).[57] The membrane curvature can be positive or negative. By convention, positive curvature refers to cases in which the membrane bulges outward away from the cytoplasm, whereas membrane bulging in the opposite direction gives rise to negative curvature (Figure 2 (a)).[57–58] In order to create a broad diversity of shapes corresponding to the specific functions, cellular membrane must undergo dynamic changes in curvature. The propensity of cellular membrane to form curved shape is characterized by the non-deformed, stress-free curvature of the membrane that is commonly referred to as the spontaneous curvature c_0.[57,59]

The concept of membrane spontaneous curvature was introduced by pioneering works of Helfrich to reflect the asymmetry between the two leaves of the bilayer.[60–61] In Helfrich's theory, inspired by the study of liquid crystals due to the fundamental physical similarity existing between lipid bilayers and nematic liquid crystals,[62] the shape of the cellular membrane is controlled by the curvature-associated bending energy

$$H = \frac{\kappa}{2} \oint \left[(c_1 + c_2 - c_0)^2 + \bar{\kappa}(c_1 \cdot c_2) \right] dA.[57,60]$$

Here, κ and $\bar{\kappa}$ denote the bending rigidity and Gaussian rigidity, respectively. It indicates that the work the cell needs to do to generate local curvature is determined by both κ and c_0, mediated by the elasticity and structure of the membrane, respectively.[57]

The importance of curvature generation as a structural feature of biological membranes has been recognized for many years, and a plethora of proteins have been identified to be involved in producing spontaneous curvature of cellular membrane utilizing different mechanisms. Extensive studies have shown that transmembrane proteins of wedge shape and peripheral proteins either inserting asymmetric amphipathic or hydrophobic structures into the bilayer or binding to the surface of one membrane monolayer generate local curvature using mechanism based on asymmetric transbilayer stress.[58,63–66] Crowding of monomeric hydrophilic
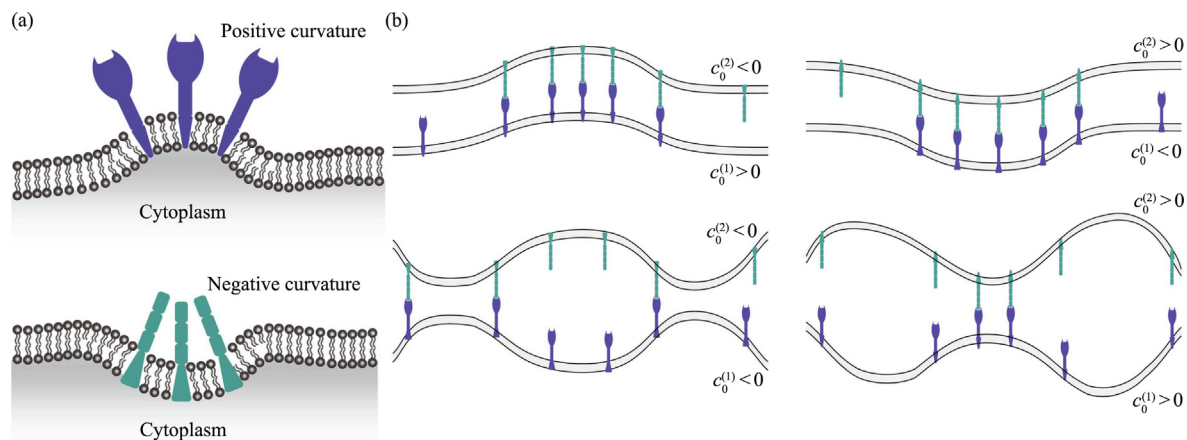
Figure 2. Local membrane curvature generated by the adhesion proteins affects the protein binding. (a) Cartoons for the generation of local membrane curvature by conical transmembrane proteins. By convention, membrane bulging outward away from the cytoplasm produces positive curvature and bulging inward negative curvature. (b) Four different combinations of protein-induced curvatures. The local curvature induced by receptors and ligands affects their binding by changing membrane deformation and inducing protein–protein interaction, depending on the combinations of the curvatures.

protein domains bound to the membrane surface has been shown *in vitro* to drive curvature due to lateral pressure generated by collisions between bound proteins.[67] Asymmetric adsorption or depletion layers of biomolecules has also been demonstrated to be an efficient way of inducing local membrane curvature attributed to depletion effect arising from the interplay between membrane flexibility and excluded volume.[68–69] These mechanisms of membrane curvature generation can certainly be utilized by the adhesion proteins. More details on mechanisms underlying the curvature generation are comprehensively summarized in the reviews.[57,63–65,70–74] There has been a flood of evidence highlighting the emerging roles for the local spontaneous curvature of membrane in many critical cellular processes such as organelle shaping,[72,75] vesicle trafficking,[76–77] cell fusion and division,[78–79] protein and lipid sorting,[80–83] as well as enzyme activation.[71,84] For example, Aimon et al. utilized FRAP to measure the membrane curvature-induced protein sorting, and found that the transmembrane protein KvAP is strongly enriched in the curved membrane tube pulled from giant unilamellar vesicles, which is attributed to protein shape and stiffness.[80] In contrast, study on the role of spontaneous curvature in the binding of membrane-anchored receptors and ligands during cell adhesion still remains at the preliminary exploration stage.

We have recently developed a mesoscopic model of membrane adhesion *via* the specific binding of curvature-inducing receptor and ligand proteins with biologically relevant parameters, in which different combinations of protein-induced curvatures are considered as shown in Figure 2 (b).[85] MC simulation results show that the local

membrane curvatures induced by the adhesion proteins do affect the receptor-ligand binding, depending on the signs of the induced curvatures. More specifically, the binding affinity K_a increases significantly with the protein-induced curvature c_0 for $-c_0^{(1)} = c_0^{(2)} = c_0$. While the opposite is true for $-c_0^{(1)} = -c_0^{(2)} = c_0$ and $c_0^{(1)} = c_0^{(2)} = c_0$. Here, $c_0^{(1)}$ and $c_0^{(2)}$ represent the local membrane curvature induced by receptors and ligands, respectively. It is found that such curvature dependence of receptor-ligand binding affinity results from the change of membrane deformations and the protein–protein *cis*-interactions due to the protein-induced curvatures.[85]

As indicated by the MC simulation results, the protein-induced curvatures change both local separation l and relative roughness $\xi_\perp$ of the two adhering membranes. For $c_0^{(1)} = c_0^{(2)} = \pm c_0$, the two adhering membranes tend to curve towards or away from each other due to the presence of induced curvature (Figure 2(b)). As a result, the average intermembrane separation $\bar{l}$ deviates from the receptor-ligand binding range with increasing protein-induced membrane curvatures, inhibiting the formation of receptor-ligand complex. And then an increase in relative membrane roughness $\xi_\perp$ is required for apposing membrane patches to locally reach the binding range *via* thermal fluctuations. For $-c_0^{(1)} = c_0^{(2)} = c_0$, the two adhering membranes tend to curve in the same direction. It is found that the induced curvature hardly affects the average intermembrane separation, but suppresses the thermally excited membrane shape fluctuations, causing a slight decrease in relative roughness $\xi_\perp$. Taking into account the effect of induced curvature on the

distribution of local membrane separations, the theoretical results based on the relation $K_a = \int K_a(l)P(l)dl$ well capture the qualitative dependence of K_a on c_0 obtained from MC simulations. However, there exist obvious quantitative difference between theoretical prediction and simulation data especially for larger c_0, thus highlighting the important contribution made by the curvature induced protein–protein *cis*-interaction, which will be discussed in detail below.

Because the bending energy of the membranes is perturbed by the presence of curvature-inducing proteins, membrane-mediated interactions between these proteins arise.[55] By modeling the proteins as disks of radius ℓ that enforce a local spontaneous curvature c_0 on the membrane, theoretical analysis revealed that the membrane-mediated pair interaction of two curvature-inducing proteins embedded in a tensionless membrane is a long-range repulsion and decays as $V(r) = 8\pi\kappa c_0^2 \ell^6 / r^4$ with r the distance between proteins.[86–89] This repulsive nature of curvature-induced protein–protein interaction results from the fact that it will lead to energetically unfavorable change in the membrane shape if two curvature-inducing proteins approach each other.[87] This curvature-induced protein–protein *cis*-repulsion can also be visualized from the pair correlation function $g(r)$ of the receptor-ligand complexes, which decreases with increasing protein-induced curvature c_0 for smaller values of r.[85] As a result of the curvature-induced protein–protein *cis*-repulsion, adhesion proteins cannot diffuse freely along the membranes with projected area of A, leading to reduced translational areas $A_\alpha = A / \left(1 + \sum_n B_{n,\alpha}[\alpha]_0^{n-1}\right)$ for receptors, ligands, as well as receptor-ligand complex. Here, $B_{n,\alpha}$ is the n-th virial coefficient, $[\alpha]_0$ is the overall concentration of each species (α = R, L or RL). Additionally incorporating the contribution of protein–protein *cis*-repulsion into the theory by taking into account the effective area for both unbound proteins and protein complexes leads to the apparent binding affinity $K = K_0 \frac{A_{BL}A}{A_R A_L}$ with $K_0 = \int K_a(l)P(l)dl$.[85] The binding affinity calculated from the theory, that simultaneously considers the curvature-induced membrane deformations and protein–protein interactions, is in good quantitative agreement with MC simulation results. These results uncover new roles of protein-induced membrane spontaneous curvature in cellular functions, and indicate that the ability to induce membrane curvatures represents a molecular property of the adhesion proteins which affects their binding kinetics and should be carefully considered in experimental characterization of the binding affinity.[85] The contribution of membrane curvature to the intercellular receptor-ligand binding remains to be tested by experiments.

Glycocalyx

In addition to the specific binders, the cells are covered by a carbohydrate-rich meshwork, termed the 'glycocalyx'.[90] Glycocalyx, also known as pericellular matrix, is mainly comprised of glycoproteins, glycolipids, proteoglycans, glycosaminoglycans, as well as associated plasma proteins.[91–92] The composition and structure of this gel-like layer, a heterogeneous mixture of proteins and lipids, change markedly depending on cell types and cell states.[93–94] Notably, the expression level of glycocalyx in cancer cells is significantly higher than in healthy cells.[95] Moreover, approximately 95 % of cancer cells have modified glycocalyx architecture.[94] Traditionally, glycocalyx is deemed to act as a physical buffer and barrier between the cell and its extracellular space,[96–97] leading to a glycocalyx-dependent entry of pathogen and nanoparticle.[90,98–99] In general, the binding receptor proteins are densely embedded in the lower strata of the cell glycocalyx.[93] Over decades, evidence has accumulated that points toward a vital role of glycocalyx environment (e.g., electrostatics, macromolecular crowding, size difference), where binding receptors reside and interact, in regulating receptor-ligand binding to control various fundamental cellular events such as stem cell differentiation, leukocyte adhesion, viral infections, as well as cancer development and progression.[90,93,100–102]

From glycoproteins bearing acidic oligosaccharides and terminal sialic acids to proteoglycans along with their associated glycosaminoglycan side chains including chondroitin sulfate, heparan sulfate, dermatan sulfate, sialic acid, and hyaluronic acid, the polyanionic nature of glycocalyx constituents imparts to it a net negative charge.[91,92,103] Acting as a semi-permeable polyelectrolyte network, the glycocalyx attracts and traps cations from the surrounding fluid reservoir, which in turn increases the concentration of ions and reduces the local pH in the glycocalyx (Figure 3). Theoretical results derived from Poisson-Boltzmann equation suggest that the electrostatic potential profile (i.e., local potential, pH, charge density) within glycocalyx is closely associated with ionic conditions, bulk pH, steric exclusion, and charge distribution.[104] Notably, theoretical model shows that even a modest sialic acid density of $2.5 \times 10^5 / \mu m^2$ within the glycocalyx can lower the cell surface pH by approximately 1 unit.[93,104] Physical forces, such as compressive force endured by cells under physiological conditions, can further reduce the pH by densifying anionic structure of glycocalyx.[93] Recent pH measurements based on the use of florescent probe, conjugated to the pH low insertion peptide, have confirmed that the pH at the surfaces of cancer cell can be fairly acidic.[105] Such electrostatic environment within the glycocalyx has important
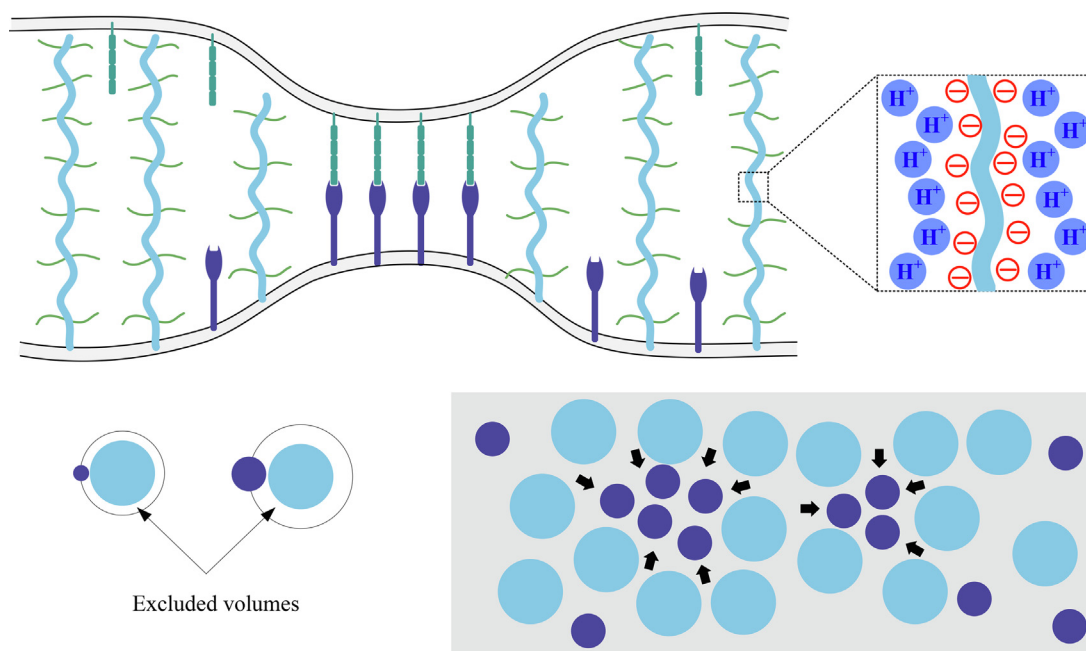
Figure 3. Cartoon of two adhering membranes in the presence of glycocalyx (in deep sky-blue). Top left: The length mismatch between binding proteins and glycocalyx leads to elastic deformation of the membranes and causes aggregation of the binding proteins, facilitating the formation of receptor-ligand complexes. Top right: Glycocalyx is negatively charged due to the polyanionic nature of its constituents. Glycocalyx attracts and traps cations from the surrounding fluid reservoir to decrease local pH and affect the intercellular receptor-ligand binding. Bottom: The glycocalyx polymers, behaving as ideal crowding agents, occupy large volumes that exclude small binding proteins (in purple) to avoid molecular overlaps (Top view). This energetically favors clustering of binding protein on the membrane to reduce total excluded volume.

implications for cell receptor function. For example, it is found that the integrin adhesion receptor ($\alpha5\beta1$) binds to its ligand (fibronectin, FA) with a pH-dependent behavior, which is required for receptor resensitization and cell migration.[106] Quantitative analysis indicates that a cell surface pH of ~ 6.1 causes more than 70 % integrins to dissociate from their ligands. Lowering the pH values to 6.0 and 5.0 from 7.5 leads to 2- and 6-fold increase in off-rate constant k_{off}, respectively.[106] Moreover, as determined by Hill coefficient, integrin-FA binding shows negative cooperativity with increasing acidity.[106] In addition, neurexin-neuroligin interactions, essential for synaptic maturation and differentiation, exhibit high affinity and show high sensitivity to ionic strength and pH conditions partially attributed to the two Ca^{2+}-binding sites at the binding interface.[11,107] Structure-based mutations by disrupting Ca^{2+} coordination at the binding interface inhibit neurexin-neuroligin interaction by increasing off-rate constant and decreasing binding affinity by up to three orders of magnitude.[107]

Generally, the glycocalyx is densely packed with biopolymers, such as mucins. At low densities, the biopolymers are not-interacting and adopt a compact mushroom-like shape. Upon increasing the biopolymer density above a threshold, these biopolymers extend away from the surface to form brushes with entropic penalty, i.e., mushroom-to-brush transition, due to steric repulsion. Similar to the thermodynamic basis of gas pressure, the entropic penalty arising from molecular crowding can generate a lateral pressure and exert entropic forces to cause the bending of anchoring membrane so that each polymer gains more conformational freedom, thus generating spontaneous membrane curvature.[67,90,108–109] Theoretical analysis indicates that the entropic pressure from anchored polymer brush and the ensuing spontaneous membrane curvature scaled monotonically with polymer coverage.[110] Recent experimental studies with mucin biopolymers have confirmed that the entropic pressure induced by this glycocalyx constituent is sufficient to generate membrane curvature, as predicted by the polymer model of membrane bending.[109] According to our previous study,[85] the induced membrane curvature by cellular glycocalyx should be involved in the intercellular receptor-ligand binding.

Another important factor within sterically crowded glycocalyx environments that should be taken into account is the 'excluded volume effect' originating from steric exclusion.[93,111] In general, the glycocalyx polymers, behaving as ideal crowding agents, occupy large volumes that exclude binding proteins to avoid molecular overlaps.[93] This crowded glyco-

calyx environment energetically favors changes that result in net reduction of total excluded volume, such as clustering and oligomerization of small binding protein on the membrane (Figure 3).[93] The induced close-packing of binding protein due to this simple physical principle is closely implicated in receptor-ligand interaction. For the 3D binding, it reveals that physiological crowding can increase the on-rate 10-fold upon dimer formation, which is attributed to the altered activation energy barrier and reaction frequency.[93,112] Accumulating evidence implies that the physiological crowding and induced protein compaction might be also a general regulatory principle in the 2D receptor-ligand binding.[9,24,100,113–115] For example, dimerization of P-selectin and PSGL-1 prolongs their bond lifetimes $(1 / k_{off})$,[100] and stabilizes cell rolling and enhances tether strength in shear flow.[116] Dimeric interactions of L-selectin-Ig and PSGL-1 show larger binding affinity as compared to the monomeric interactions with monomeric PSGL-1.[115] In addition, 2D *in situ* kinetic measurements suggest that the association of TCRs into nanoclusters leads to enhanced binding kinetics of TCR-pMHC interactions, which enable T cells to efficiently recognize rare antigens and promote T cell signaling.[9,24,113] Recently, Vu et al. utilized fluorescence technique and adhesion frequency measurements to show that P120 catenin potentiates constitutive E-cadherin dimerization at the plasma membrane, which in turn increases the cadherin 2D *trans* binding affinity and off-rate constant.[114]

The thickness of glycocalyx layer, depending on cell type and cell states, in general ranges from tens to hundreds of nanometers, thus typically burying even large binding proteins.[96,117] This size difference imposes physical constraints on the probability of forming successful receptor-ligand complexes. Consistent with expectations, Lorz et al. analyzed the adhesion of giant vesicles decorated with sialyl-Lewis^X ligands and lipopolymers to E-selectin functionalized substrate and revealed that the receptor-ligand binding affinity decreases in the presence lipopolymers.[102] Moreover, Mulivor and Lipowsky found that removal of the glycocalyx with heparinase increases receptor-ligand binding affinity and enhances leukocyte-endothelial cell adhesion.[101] Perturbations to components such as sialic acids, HA and mucins that increase the spacing of apposing surface or stiffen the glycocalyx[118–119] makes it harder for the receptors to reach ligands and tends to pull apart receptor-ligand complexes when they form, which in turn alters binding affinities by several orders of magnitude.[120–121]

In addition to acting as steric barrier due to the mismatch in size, the glycocalyx can also lead to aggregation of binding proteins on the membrane (Figure 3). A physical picture is that the size difference leads to a membrane-mediated repulsion between the glycocalyx and receptor-ligand complexes, simply because the lipid membranes have to be bent to compensate for the size mismatch, which costs elastic energy.[122] As a consequence of this membrane-mediated repulsion, the binding proteins and glycocalyx tend to segregate from one another. This mechanism based on the mismatch in size has been proposed to underlie characteristic molecular organization of the immunological synapse during T cell adhesion.[8,122] Using giant unilamellar vesicles decorated with synthetic binding and non-binding proteins, Schmid et al. confirmed the size-dependent protein segregation at membrane interfaces.[123] Further, the principle of size-induced protein segregation as an organizing force in the cancer glycocalyx has also been demonstrated for integrin adhesion receptors.[93,120] The glycocalyx-mediated integrin clustering locally increases binding affinity and kinetic rates by virtue of cooperative binding, which facilitates focal adhesions and promotes integrin-dependent cell growth and survival.[120]

Many types of receptor-ligand interactions exhibit force-dependent kinetics. For example, the lifetime $(1 / k_{off})$ of the slip bond (e.g., biotin-streptavidin bond) decreases when being pulled apart by an external tensile force.[124] In contrast, a catch bond (e.g., TCR-pMHC bond) shows a force-enhanced lifetime.[125–126] Due to the mismatch in size, compression of the glycocalyx by short receptor-ligand bonds gives rise to an equal and opposite tensile force on the bonds. This applied force acting on the bonds should reasonably be involved in the regulation of receptor-ligand interactions. Consistent with this expectation, Paszek et al. demonstrated that the bulky glycocalyx physically alters integrin state by applying tension to the integrin-ligand bonds to induce conformational changes that would activate integrins.[120] This altered integrin state, which determines integrin-ligand binding kinetics, promote the growth factor signalling pathways to support cell growth and survival. These results in this section highlight the multiple roles of glycocalyx in the receptor-ligand binding, and can provide more potential targets for the development of novel drugs and therapeutic interventions.

Lipid Raft

In the aforementioned studies, the biomembrane is often viewed as a fluid bilayer with homogeneous distribution of lipids and proteins as proposed by Singer and Nicolson 50 years ago.[127] The paradigm of biomembranes has gone through a major update.[128] Cumulative evidence suggests that the biomembranes are, instead of structurally homogeneous, multicomponent and heterogeneous supramolecular systems, consisting of fluctuating nanoscale microdomains enriched in saturated phospholipids and cholesterol.[129–136] These microdomains, termed as lipid rafts, exist as distinct

liquid-ordered phases that diffuse in the liquid-disordered matrix of the plasma membrane.[137–138] The lipid rafts have larger rigidity and hydrophobic thickness than the membrane matrix[139–140] and undergo highly dynamic merging and fission attributed to, e.g., actin cytoskeleton rearrangement, protein-lipid and protein–protein interactions.[141–144] In addition, lipid rafts often exhibit less fluidity than the surrounding membranes, due to the compact packing of the hydrophobic chains of saturated lipids.[145–146] Theses dynamic microdomains are involved in nearly all aspects of mammalian membrane physiology,[147] and play a central role in many cellular processes, including signal transduction and membrane trafficking.[148] Extensive studies have demonstrated a close correlation between lipid rafts and neurodegenerative disease, cancer, cardiovascular diseases, prion diseases, autoimmune diseases and viral infection.[148–149] This makes these specific microdomains, which have been receiving increasing attention, a promising target for pharmacological treatment of these diseases.

One of the most intriguing properties of lipid rafts is that they can selectively recruit and retain specific proteins to variable extents (i.e., raft affinity), leading to a heterogeneous distribution of proteins in the membranes.[150] The basis for protein partitioning into lipid rafts remains a largely unanswered question in membrane biology.[151] The physical features of protein transmembrane domains including surface area, length, and palmitoylation are identified as structural determinants of raft affinity to transmembrane proteins.[147] A wide number of signaling and adhesion proteins, such as TCR and CD44, have been demonstrated to be closely associated with lipid rafts.[150,152–153] Functionally, lipid rafts are believed to serve as sorting and signaling platforms that contribute to specific protein–protein interactions on a single membrane (*cis*-interaction) by virtue of spatial proximity and selective recruitment of participating components, thereby facilitating efficiency and specificity of signal transduction cascades.+.[150,154–155]

In addition to the *cis*-interaction, existing studies indicate that lipid rafts have an impact on *trans* intercellular receptor-ligand interaction as well. *In situ* experiments show that lipid rafts help the binding of TCR to pMHC anchored on antigen presenting cell membrane and T cell activation due to the aggregation of raft-associated pMHC molecules into these microdomains.[156–157] Disrupting the lipid rafts in T cell membrane *via* cholesterol depletion with methyl-beta-cyclodextrin (MβCD) directly was found to reduce the TCR-pMHC binding affinity K_a and off-rate k_{off}, highlighting the importance of signaling protein-raft association for TCR-pMHC binding kinetics.[9] Similarly, experiments of mimetic systems composed of giant vesicles decorated with biotin adhering to streptavidin-functionalized supported bilayers show that destabilizing raft and protein heterogeneities in vesicles

by MβCD adversely affects the biotin-streptavidin binding and stable adhesion.[158–159]

To elucidate the mechanism underlying the raft-dependent intercellular receptor-ligand binding, we systematically investigate the role of lipid raft in the receptor-ligand binding using Monte Carlo simulations of multicomponent membrane adhesion model with biologically relevant parameters.[56,144,154,160–161] Within the framework of classical statistical mechanics, it is found that the binding affinity of membrane-anchored receptors and ligands is enhanced when the adhesion molecules preferentially partition into lipid rafts, consistent with the experimental observation.[9] Such enhancement is shown to be sensitive to raft characteristics including area fraction, size, raft-raft contact energy, as well as raft affinity to proteins. Especially, a dramatical increase in K_a coincides with the phase transition from homogeneous state to phase-separated state by regulating raft-raft contact energy, regardless of the specific values of model parameters. The binding affinity K_a therefore represents a general indicator of the phase transition in the multicomponent membrane adhesion system. This enhancement in binding affinity by the presence of lipid raft can be attributed to the entropy gain of the membranes resulting from raft-induced protein aggregation (Figure 4).[154] More specifically, on the one hand, the effective increase in concentrations of binding proteins due to raft affinity amplifies the receptor-ligand binding rate, which in turn elevates the K_a. On the other hand, aggregation of binding proteins in lipid rafts smoothens out the membranes locally, which facilitates the cooperative binding of receptors and ligands.[160] Because the proteins preferentially partition into the lipid raft domains in the membranes, the overall membranes can take more configurations by having more complexes within rafts.[154] Contrary to the case of homogeneous membranes where the binding affinity of membrane-anchored receptor and ligand is weakened by the thermally excited membrane shape fluctuations,[7] the membrane roughness resulting from shape fluctuations on nanoscales makes a positive contribution to the receptor-ligand binding in collaboration with lipid rafts. The bending rigidity contrast between lipid rafts and non-raft region suppresses the local thermal fluctuation within raft domains and facilitates raft clustering and protein aggregation, which in turn further increases receptor-ligand binding affinity.

The receptors or ligands may experience *cis* interactions due to electrostatics. Recent studies of cell adhesion on a supported lipid bilayer functionalized with ligand proteins suggest that the *cis*-interaction affects the function of lipid raft in *trans* receptor-ligand interaction.[56] For the adhesion system with attractive ligand–ligand *cis*-interactions, it helps lipid raft and protein molecules to aggregation, which further increases receptor-ligand binding affinity K_a due to enhanced coopera-

(a) Without lipid rafts

(b) Small raft-raft contact energy

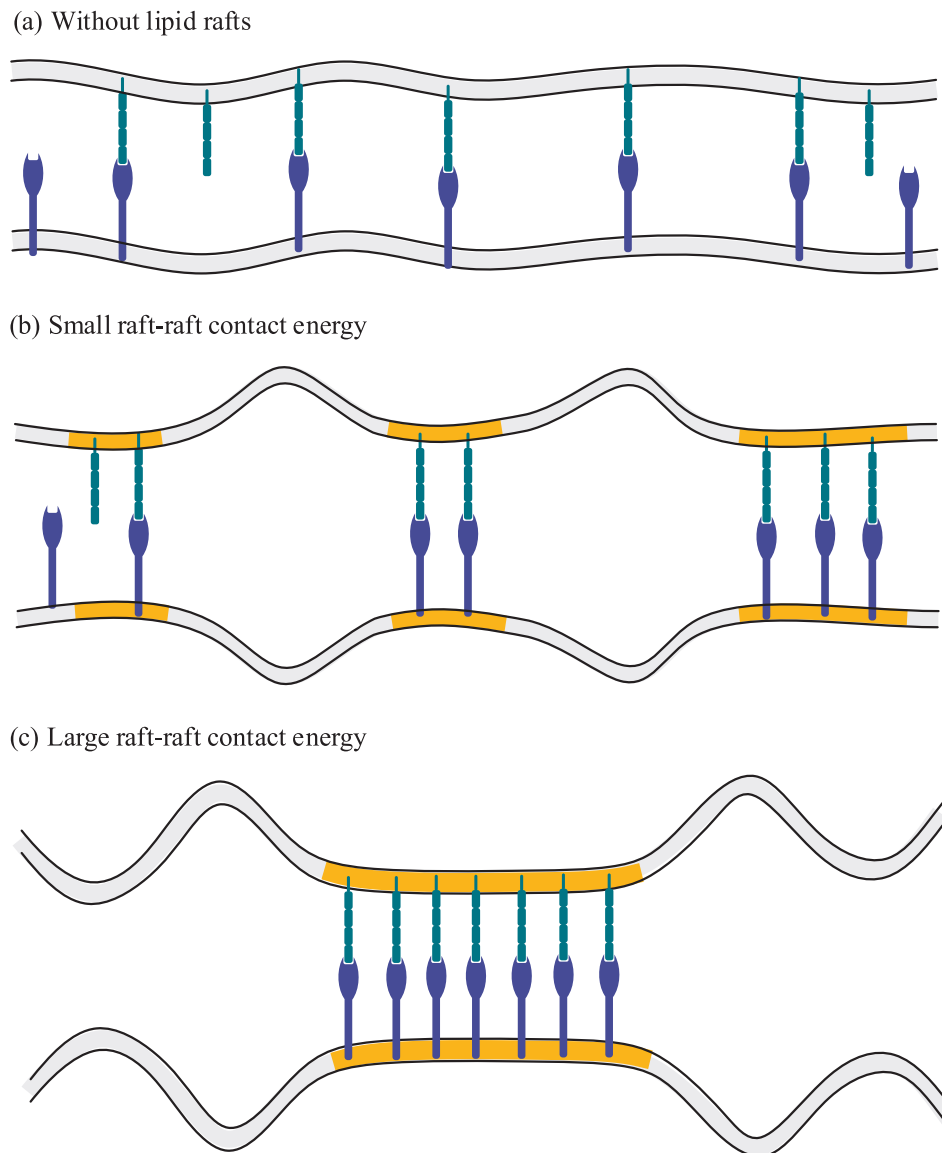(c) Large raft-raft contact energy

Figure 4. Illustration of the effect of lipid raft (in orange) on the intercellular receptor-ligand binding. The lipid rafts tend to coalesce partially due to the hydrophobic mismatch between the rafts and the membrane matrix. By virtue of the raft affinity to the receptors and ligands, lipid rafts lead to the protein aggregation, which in turn contributes to the receptor-ligand binding. This enhancement in receptor-ligand binding by the presence of lipid raft can be attributed to the conformational entropy gain of the fluctuating membranes.

tive binding and more entropy gain of the cell membranes. Conversely, the repulsive ligand–ligand *cis*-interactions negatively affect the receptor-ligand binding by suppressing the protein aggregation and thermal shape fluctuations of cell membrane. In contrast to the case of attractive *cis*-interaction, coalescence of lipid rafts may function as a negative regulator for the receptor-ligand binding. This effect can be explained as follows. Raft-associated receptors tend to aggregate due to lipid rafts coalescence in cell membrane, which can lead to excessive free receptors in raft domains by the presence of ligand–ligand repulsion. In order to bind with the unbound ligands outside of the region apposing the raft

domains, the excessive free receptors localized in raft domains have to overcome the raft affinity.[161] This energetic penalty gives rise to a decrease in binding affinity. These studies in this section extend and deepen our understanding of how the raft-based membrane heterogeneity functions in receptor-ligand interactions, and could inspire new the therapeutic strategies targeting receptor-ligand interactions in diseases.

Biomedical Significances

Studies on the functional role of protein-membrane interaction in the receptor-ligand

binding have provided routes and strategies for novel therapies. First, take for example the glycocalyx, which has received increasing attention because of its implication in, e.g., cancer metastasis, inflammatory processes, platelet and leucocyte adhesion by affecting intercellular receptor-ligand binding.[162–164] A new therapeutic strategy aimed at intervening the intercellular receptor-ligand binding between natural killer cell and cancer cell by precision glycocalyx editing with an antibody-enzyme conjugate potentiates NK cell killing by antibody-dependent cell-mediated cytotoxicity, therefore providing a promising avenue for cancer immune therapy.[162] Circulating tumor cells (CTCs), namely tumor cells invade into the blood vessel and circulate through the vascular system, contribute to the spread of cancer metastasis and have emerged as a promising prognostic biomarker. Disrupting and remodeling the glycocalyx by, e.g., changing shear stress, inflammatory conditions, and matrix metalloproteinase exposure, increase the receptor number available to interact with CTC ligands and receptor-ligand binding affinity, thus hindering the vascular transport of CTCs to distant organs and preventing the onset of metastasis.[163] This approach provides a powerful complement to the existing CTC therapeutic strategies involving E-selectin targeting and TRAIL-induced apoptosis.[163] In addition, a range of cardiovascular disorders have been demonstrated to be related to pathological glycocalyx shedding, which gives rise to endothelial dysfunction and inflammation. Therapeutic strategies designed to regulate receptor-ligand binding affinity and cell adhesion by restoring the endothelial glycocalyx show promising potentials to avoid cardiovascular disease initiation and progression.[164] These studies suggest that therapeutic interventions aiming at disrupting or restoring the glycocalyx may be disease specific.

Lipid raft, as a potential therapeutic agent for the treatment of a broad range of diseases, has also been widely studied. A considerable body of evidence indicates that lipid rafts are involved in migration and invasion of metastatic cancer cells by regulating receptor-ligand binding.[152,165] Moreover, lipid rafts can affect, e.g., TCR-pMHC binding to regulate function and response of immune cells including macrophages and T cells, which are vital for anti-tumor immunity.[166] These findings have turned lipid rafts into promising targets in anticancer therapy. It has become evident that lipid rafts have a significant impact on the binding and entry of different viruses to host cells, including human immunodeficiency virus (HIV) and coronaviruses. For the syndrome coronavirus-2 (SARS-CoV-2), it has been revealed that lipid rafts provide a functional platform able to localize angiotensin-converting enzyme-2 (ACE-2), the main receptor for SARS-CoV-2, on the host cell membrane, which facilitates the interaction of ACE-2 with the spike protein on viral envelope.[167] Disrupting lipid raft by cholesterol-depletion with, e.g., MβCD, stains, and cyclodextrins can lead to reduced coronavirus adhesion, entry, as well as infectivity by impairing the ACE-2-spike interaction.[167] These encouraging results introduce a potential new task and opportunity in the pharmacological therapeutic approach against coronavirus that currently ravages the world. In addition, in view of the prominent role of lipid raft in neuronal cell adhesion mediated by raft-associated neural cell adhesion molecule (NCAM), which is implicated in neuronal synapse formation, maintenance, and function, as well as astrocyte-neuron interactions,[168–169] targeting lipid raft and homophilic NCAM interaction may further motivate fruitful therapeutic approaches for neurological diseases.

Discussion and Perspective

Cells interact with their immediate neighbors to sense, respond and adapt to outside world *via* the specific binding of receptors and ligands anchored on the two apposing membranes. Because of its great potential to stimulate new therapeutic targets in drug design and promote disease prevention and treatment, the intercellular receptor-ligand binding has received considerable attention. In sharp contrast to the 3D protein binding, the intercellular receptor-ligand binding that occurs in 2D is sensitive to the membrane environment due to the protein-membrane interactions, requiring more in-depth investigations to illuminate the underlying mechanisms. In this review, we summarize the advances regarding the regulatory effects on the intercellular receptor-ligand binding mainly from four aspects: (1) membrane fluctuations, (2) membrane curvature, (3) glycocalyx, (4) lipid raft, in which the fundamental mechanisms based on average intermembrane separation, relative membrane roughness, protein–protein *cis*-interactions, protein aggregation are elucidated. These studies deepen our understanding regarding the prominent role of protein-membrane interaction in the intercellular receptor-ligand binding and contribute to drug design and disease treatment by bringing to light new therapeutic targets.

Recently, the impact of bioelectric microenvironment (e.g., membrane potential, ion flux, charged lipid component) on the intercellular receptor-ligand binding has become a pressing issue to be solved. Especially for neurons, their neuronal activities including synapse formation, function and elimination all depend strongly on the dynamic action potential.[170–173] Existing studies have confirmed the involvement of membrane potential in the receptor-ligand interactions. Take for example the G-protein coupled receptors (GPCRs), the largest family of human membrane proteins serving as primary targets of

approximately-one third of currently marketed drugs.[174] Experimental and simulation results indicate that GPCRs can sense the change in membrane potential and exhibit a voltage-dependent binding to their soluble ligands.[175–176] An underlying mechanism is proposed that the membrane potential induces conformational alterations inside the transmembrane domains of GPCRs, thereby influencing their binding affinity for soluble extracellular ligands.[175] This regulatory strategy based on voltage-induced conformational change would potentially be utilized as a general principle to regulate the intercellular binding of adhesion GPCRs to ligands anchored on pre-synaptic membrane and other types of receptors and ligands (e.g., NCAM),[177] which needs to be further verified.

Although the regulatory factors discussed above are often investigated separately in individual studies, they are not mutually exclusive but instead work together in the intercellular receptor-ligand binding under physiological conditions. Therefore, to obtain a comprehensive understanding of intercellular receptor-ligand binding for the discovery of safer and more effective drugs, further studies on coupling effect of these regulatory factors based on more complicated multiparameter systems are needed. More in-depth researches will continue to provide guidelines and strategies for clinically effective drugs.

CRediT authorship contribution statement

Long Li: Conceptualization, Funding acquisition, Investigation, Software, Visualization, Writing – original draft, Writing – review & editing. **Jing Ji:** Conceptualization, Funding acquisition, Project administration, Supervision, Writing – original draft, Writing – review & editing. **Fan Song:** Funding acquisition, Resources, Writing – review & editing. **Jinglei Hu:** Conceptualization, Funding acquisition, Investigation, Project administration, Resources, Supervision, Visualization, Writing – original draft, Writing – review & editing.

DATA AVAILABILITY

No data was used for the research described in the article.

References

1. Su, X.L., Ditlev, J.A., Hui, E.F., Xing, W.M., Banjade, S., Okrut, J., (2016). Phase separation of signaling molecules promotes T cell receptor signal transduction. *Science* **352**, 595–599.

2. Wang, J., Sun, J.W., Liu, L.N., Flies, D.B., Nie, X.X., Toki, M., (2019). Siglec-15 as an immune suppressor and potential target for normalization cancer immunotherapy. *Nat Med* **25**, 656–666.

3. Newton, R.H., Shrestha, S., Sullivan, J.M., Yates, K.B., Compeer, E.B., Ron-Harell, N., (2018). Maintenance of CD4 T cell fitness through regulation of Foxo1. *Nat Immunol* **19**, 838–848.

4. Giampazolias, E., Schulz, O., Lim, K.H.J., Rogers, N.C., Chakravarty, P., Srinivasan, N., (2021). Secreted gelsolin inhibits DNGR-1-dependent cross-presentation and cancer immunity. *Cell* **184**, 1–16.

5. Cai, E., Marchuk, K., Beemiller, P., Beppler, C., Rubashkin, M.G., Weaver, V.M., (2017). Visualizing dynamic microvillar search and stabilization during ligand detection by T cells. *Science* **356**, eaal3118.

6. Xiong, G.F., Chen, J., Zhang, G.Y., Wang, S.K., Kawasaki, K., Zhu, J.Q., (2020). Hsp47 promotes cancer metastasis by enhancing collagen-dependent cancer cell-platelet interaction. *Proc Natl Acad Sci U S A* **117**, 3748–3758.

7. Hu, J.L., Lipowsky, R., Weikl, T.R., (2013). Binding constants of membrane-anchored receptors and ligands depend strongly on the nanoscale roughness of membranes. *Proc Natl Acad Sci U S A* **110**, 15283–15288.

8. Li, L., Hu, J.L., Rozycki, B., Wang, X.H., Wu, H.L., Song, F., (2021). Influence of lipid rafts on pattern formation during T-cell adhesion. *New J Phys* **23**, 043052

9. Huang, J., Zarnitsyna, V.I., Liu, B.Y., Edwards, L.J., Jiang, N., Evavold, B.D., (2010). The kinetics of two-dimensional TCR and pMHC interactions determine T-cell responsiveness. *Nature* **464**, 932–936.

10. Ledda, F., (2007). Ligand-induced cell adhesion as a new mechanism to promote synapse formation. *Celll Adhes Migr* **1**, 137–139.

11. Leone, P., Comoletti, D., Ferracci, G., Conrod, S., Garcia, S.U., Taylor, P., (2010). Structural insights into the exquisite selectivity of neurexin/neuroligin synaptic interactions. *Embo J* **29**, 2461–2471.

12. Czondor, K., Garcia, M., Argento, A., Constals, A., Breillat, C., Tessier, B., (2013). Micropatterned substrates coated with neuronal adhesion molecules for high-content study of synapse formation. *Nat Commun* **4**, 2252.

13. Ko, J., Fuccillo, M.V., Malenka, R.C., Sudhof, T.C., (2009). LRRTM2 functions as a neurexin ligand in promoting excitatory synapse formation. *Neuron* **64**, 791–798.

14. Lee, K., Kim, Y., Lee, S.J., Qiang, Y., Lee, D., Lee, H.W., (2013). MDGAs interact selectively with neuroligin-2 but not other neuroligins to regulate inhibitory synapse development. *Proc Natl Acad Sci U S A* **110**, 336–341.

15. Craig, A.M., Kang, Y., (2007). Neurexin-neuroligin signaling in synapse development. *Curr Opin Neurobiol* **17**, 43–52.

16. Kim, J.A., Kim, D., Won, S.Y., Han, K.A., Park, D., Cho, E., (2017). Structural insights into modulation of neurexin-neuroligin trans-synaptic adhesion by MDGA1/neuroligin-2 complex. *Neuron* **94**, 1121–1131.

17. Dustin, M.L., Bromley, S.K., Davis, M.M., Zhu, C., (2001). Identification of self through two-dimensional chemistry and synapses. *Annu Rev Cell Dev Biol* **17**, 133–157.

18. Dinamarca, M.C., Rios, J.A., Inestrosa, N.C., (2012). Postsynaptic receptors for arnyloid-beta oligomers as mediators of neuronal damage in Alzheimer's disease. *Front Physiol* **3**, 464.

19. Sindi, I.A., Dodd, P.R., (2015). New insights into Alzheimer's disease pathogenesis: the involvement of neuroligins in synaptic malfunction. *Neurodegener Dis Manag* **5**, 137–145.

20. Zhang, W.T., Huang, Q.H., Xiao, W.W., Zhao, Y., Pi, J., Xu, H., (2020). Advances in anti-tumor treatments targeting the CD47/SIRPα axis. *Front Immunol* **11**, 18.

21. Ring, N.G., Herndler-Brandstetter, D., Weiskopf, K., Shan, L., Volkmer, J.P., George, B.M., (2017). Anti-SIRPα antibody immunotherapy enhances neutrophil and macrophage antitumor activity. *Proc Natl Acad Sci U S A* **114**, E10578–E10585.

22. Weiskopf, K., (2017). Cancer immunotherapy targeting the CD47/SIRPα axis. *Eur J Cancer* **76**, 100–109.

23. Logtenberg, M.E.W., Scheeren, F.A., Schumacher, T.N., (2020). The CD47-SIRPα immune checkpoint. *Immunity* **52**, 742–752.

24. Huang, J., Meyer, C., Zhu, C., (2012). T cell antigen recognition at the cell membrane. *Mol Immunol* **52**, 155–164.

25. Davis, M.M., Boniface, J.J., Reich, Z., Lyons, D., Hampl, J., Arden, B., (1998). Ligand recognition by αβ T cell receptors. *Annu Rev Immunol* **16**, 523–544.

26. Gascoigne, N.R., Zal, T., Alam, S.M., (2001). T-cell receptor binding kinetics in T-cell development and activation. *Expert Rev Mol Med* **2001**, 1–17.

27. Matsui, K., Boniface, J.J., Steffner, P., Reay, P.A., Davis, M.M., (1994). Kinetics of T-cell receptor-binding to peptide I-E^k complexes: Correlation of the dissociation rate with T-cell responsiveness. *Proc Natl Acad Sci U S A* **91**, 12862–12866.

28. van der Merwe, P.A., (2001). The TCR triggering puzzle. *Immunity* **14**, 665–668.

29. Steinkühler, J., Rozycki, B., Alvey, C., Lipowsky, R., Weikl, T.R., Dimova, R., (2019). Membrane fluctuations and acidosis regulate cooperative binding of 'marker of self' protein CD47 with the macrophage checkpoint receptor SIRPα. *J Cell Sci* **132**, jcs216770.

30. Huppa, J.B., Axmann, M., Mortelmaier, M.A., Lillemeier, B.F., Newell, E.W., Brameshuber, M., (2010). TCR-peptide-MHC interactions in situ show accelerated kinetics and increased affinity. *Nature* **463**, 963–U143.

31. O'Donoghue, G.P., Pielak, R.M., Smoligovets, A.A., Lin, J.J., Groves, J.T., (2013). Direct single molecule measurement of TCR triggering by agonist pMHC in living primary T cells. *Elife* **2**, e00778.

32. Tolentino, T.P., Wu, J.H., Zarnitsyna, V.I., Fang, Y., Dustin, M.L., Zhu, C., (2008). Measuring diffusion and binding kinetics by contact area FRAP. *Biophys J* **95**, 920–930.

33. Liu, B.Y., Chen, W., Evavold, B.D., Zhu, C., (2014). Accumulation of dynamic catch bonds between TCR and agonist peptide-MHC triggers T cell signaling. *Cell* **157**, 357–368.

34. Liu, B.Y., Zhong, S., Malecek, K., Johnson, L.A., Rosenberg, S.A., Zhu, C., (2014). 2D TCR-pMHC-CD8 kinetics determines T-cell responses in a self-antigen-specific TCR system. *Eur J Immunol* **44**, 239–250.

35. Zhang, M.M., Wang, B., Xu, B.Q., (2014). Mapping single molecular binding kinetics of carbohydrate-binding module with crystalline cellulose by atomic force microscopy recognition imaging. *J Phys Chem B* **118**, 6714–6720.

36. Muller, D.J., Dufrene, Y.F., (2008). Atomic force microscopy as a multifunctional molecular toolbox in nanobiotechnology. *Nat Nanotechnol* **3**, 261–269.

37. Doan, T.L.L., Guerardel, Y., Loubiere, P., Mercier-Bonin, M., Dague, E., (2011). Measuring kinetic dissociation/association constants between Lactococcus lactis bacteria and mucins using living cell probes. *Biophys J* **101**, 2843–2853.

38. Li, Q.H., Wayman, A., Lin, J.G., Fang, Y., Zhu, C., Wu, J.H., (2016). Flow-enhanced stability of rolling adhesion through E-selectin. *Biophys J* **111**, 686–699.

39. Limozin, L., Bongrand, P., Robert, P., (2016). A rough energy landscape to describe surface-linked antibody and antigen bond formation. *Sci Rep* **6**, 35193.

40. Paschall, C.D., Guilford, W.H., Lawrence, M.B., (2008). Enhancement of L-selectin, but not P-selectin, bond formation frequency by convective flow. *Biophys J* **94**, 1034–1045.

41. Edwards, L.J., Zarnitsyna, V.I., Hood, J.D., Evavold, B.D., Zhu, C., (2012). Insights into T cell recognition of antigen: significance of two-dimensional kinetic parameters. *Front Immunol* **3**, 86.

42. Krogsgaard, M., Prado, N., Adams, E.J., He, X.L., Chow, D.C., Wilson, D.B., (2003). Evidence that structural rearrangements and/or flexibility during TCR binding can contribute to T cell activation. *Mol Cell* **12**, 1367–1378.

43. Krobath, H., Rozycki, B., Lipowsky, R., Weikl, T.R., (2009). Binding cooperativity of membrane adhesion receptors. *Soft Matter* **5**, 3354–3361.

44. Freund, L.B., (2013). Entropic pressure between biomembranes in a periodic stack due to thermal fluctuations. *Proc Natl Acad Sci U S A* **110**, 2047–2051.

45. Li, L., Wang, X.H., Shao, Y.F., Li, W., Song, F., (2018). Entropic pressure between fluctuating membranes in multilayer systems. *Sci China-Phys Mech Astron* **61**, 128711

46. Li, L., Song, F., (2018). *Undulation force between membranes Adv Mech* **48**, 438–460.

47. Li, L., Song, F., (2016). Entropic force between biomembranes. *Acta Mech Sin* **32**, 970–975.

48. Fenz, S.F., Bihr, T., Schmidt, D., Merkel, R., Seifert, U., Sengupta, K., (2017). Membrane fluctuations mediate lateral interaction between cadherin bonds. *Nat Phys* **13**, 906–913.

49. Bruinsma, R., Goulian, M., Pincus, P., (1994). Self-assembly of membrane junctions. *Biophys J* **67**, 746–750.

50. Yuan, H.Y., Gao, H.J., (2012). On the mechanics of integrin clustering during cell-substrate adhesion. *Acta Mech Solida Sin* **25**, 467–472.

51. Marzban, B., Yuan, H.Y., (2017). The effect of thermal fluctuation on the receptor-mediated adhesion of a cell membrane to an elastic substrate. *Membranes* **7**, 24.

52. Xu, G.K., Hu, J.L., Lipowsky, R., Weikl, T.R., (2015). Binding constants of membrane-anchored receptors and ligands: A general theory corroborated by Monte Carlo simulations. *J Chem Phys* **143**, 243136

53. Hu, J.L., Xu, G.K., Lipowsky, R., Weikl, T.R., (2015). Binding kinetics of membrane-anchored receptors and ligands: Molecular dynamics simulations and theory. *J Chem Phys* **143**, 243137

54. Weikl, T.R., Hu, J.L., Xu, G.K., Lipowsky, R., (2016). Binding equilibrium and kinetics of membrane-anchored receptors and ligands in cell adhesion: Insights from computational model systems and theory. *Cell Adhes Migr* **10**, 576–589.

55. Weikl, T.R., (2018). Membrane-mediated cooperativity of proteins. *Annu Rev Phys Chem* **69**, 521–539.

56. Li, L., Hu, J.L., Wu, H.P., Song, F., (2021). Cis-interaction of ligands on a supported lipid bilayer affects their binding to cell adhesion receptors. *Sci China-Phys Mech Astron* **64**, 108712

57. Zimmerberg, J., Kozlov, M.M., (2006). How proteins produce cellular membrane curvature. *Nat Rev Mol Cell Biol* **7**, 9–19.

58. Johannes, L., Wunder, C., Bassereau, P., (2014). Bending "on the rocks"-a cocktail of biophysical modules to build endocytic pathways. *Cold Spring Harbor Perspect Biol* **6**, a016741

59. Lanigan, P.M.P., Chan, K., Ninkovic, T., Templer, R.H., French, P.M.W., de Mello, A.J., (2008). Spatially selective sampling of single cells using optically trapped fusogenic emulsion droplets: a new single-cell proteomic tool. *J R Soc Interface* **5**, S161–S168.

60. Helfrich, W., (1973). Elastic properties of lipid bilayers - theory and possible experiments. *Z Naturforsch* **28c**, 693–703.

61. Miao, L., Seifert, U., Wortis, M., Dobereiner, H.G., (1994). Budding transitions of fluid-bilayer vesicles: the effect of area-difference elasticity. *Phys Rev E* **49**, 5389–5407.

62. Bassereau, P., Jin, R., Baumgart, T., Deserno, M., Dimova, R., Frolov, V.A., (2018). The 2018 biomembrane curvature and remodeling roadmap. *J Phys D-Appl Phys* **51**, 343001

63. McMahon, H.T., Gallop, J.L., (2005). Membrane curvature and mechanisms of dynamic cell membrane remodelling. *Nature* **438**, 590–596.

64. Baumgart, T., Capraro, B.R., Zhu, C., Das, S.L., (2011). Thermodynamics and mechanics of membrane curvature generation and sensing by proteins and lipids. *Annu Rev Phys Chem* **62**, 483–506.

65. Ramakrishnan, N., Kumar, P.B.S., Radhakrishnan, R., (2014). Mesoscale computational studies of membrane bilayer remodeling by curvature-inducing proteins. *Phys Rep* **543**, 1–60.

66. Kozlov, M.M., Campelo, F., Liska, N., Chernomordik, L.V., Marrink, S.J., McMahon, H.T., (2014). Mechanisms shaping cell membranes. *Curr Opin Cell Biol* **29**, 53–60.

67. Stachowiak, J.C., Schmid, E.M., Ryan, C.J., Ann, H.S., Sasaki, D.Y., Sherman, M.B., (2012). Membrane bending by protein-protein crowding. *Nat Cell Biol* **14**, 944–949.

68. Rozycki, B., Lipowsky, R., (2015). Spontaneous curvature of bilayer membranes from molecular simulations: Asymmetric lipid densities and asymmetric adsorption. *J Chem Phys* **142**, 054101

69. Rozycki, B., Lipowsky, R., (2016). Membrane curvature generated by asymmetric depletion layers of ions, small molecules, and nanoparticles. *J Chem Phys* **145**, 074117

70. McMahon, H.T., Boucrot, E., (2015). Membrane curvature at a glance. *J Cell Sci* **128**, 1065–1070.

71. Iversen, L., Mathiasen, S., Larsen, J.B., Stamou, D., (2015). Membrane curvature bends the laws of physics and chemistry. *Nat Chem Biol* **11**, 822–825.

72. Shibata, Y., Hu, J.J., Kozlov, M.M., Rapoport, T.A., (2009). Mechanisms shaping the membranes of cellular organelles. *Annu Rev Cell Dev Biol* **25**, 329–354.

73. Stachowiak, J.C., Brodsky, F.M., Miller, E.A., (2013). A cost-benefit analysis of the physical mechanisms of membrane curvature. *Nat Cell Biol* **15**, 1019–1027.

74. Graham, T.R., Kozlov, M.M., (2010). Interplay of proteins and lipids in generating membrane curvature. *Curr Opin Cell Biol* **22**, 430–436.

75. Wang, N., Clark, L.D., Gao, Y., Kozlov, M.M., Shemesh, T., Rapoport, T.A., (2021). Mechanism of membrane-curvature generation by ER-tubule shaping proteins. *Nat Commun* **12**, 568.

76. Lee, M.C.S., Orci, L., Hamamoto, S., Futai, E., Ravazzola, M., Schekman, R., (2005). Sar1p N-terminal helix initiates membrane curvature and completes the fission of a COPII vesicle. *Cell* **122**, 605–617.

77. Beck, R., Sun, Z., Adolf, F., Rutz, C., Bassler, J., Wild, K., (2008). Membrane curvature induced by Arf1-GTP is essential for vesicle formation. *Proc Natl Acad Sci U S A* **105**, 11731–11736.

78. Smith, J.A., Hall, A.E., Rose, M.D., (2017). Membrane curvature directs the localization of Cdc42p to novel foci required for cell-cell fusion. *J Cell Biol* **216**, 3971–3980.

79. Beltran-Heredia, E., Almendro-Vedia, V.G., Monroy, F., Cao, F.J., (2017). Modeling the mechanics of cell division: influence of spontaneous membrane curvature, surface tension, and osmotic pressure. *Front Physiol* **8**, 312.

80. Aimon, S., Callan-Jones, A., Berthaud, A., Pinot, M., Toombes, G.E.S., Bassereau, P., (2014). Membrane shape modulates transmembrane protein distribution. *Dev Cell* **28**, 212–218.

81. Sorre, B., Callan-Jones, A., Manneville, J.B., Nassoy, P., Joanny, J.F., Prost, J., (2009). Curvature-driven lipid sorting needs proximity to a demixing point and is aided by proteins. *Proc Natl Acad Sci U S A* **106**, 5622–5626.

82. Zhu, C., Das, S.L., Baumgart, T., (2012). Nonlinear sorting, curvature generation, and crowding of endophilin N-BAR on tubular membranes. *Biophys J* **102**, 1837–1845.

83. Vanni, S., Hirose, H., Barelli, H., Antonny, B., Gautier, R., (2014). A sub-nanometre view of how membrane curvature and composition modulate lipid packing and protein recruitment. *Nat Commun* **5**, 4916.

84. Bohr, S.S.R., Thorlaksen, C., Kuhnel, R.M., Gunther-Pomorski, T., Hatzakis, N.S., (2020). Label-free fluorescence quantification of hydrolytic enzyme activity on native substrates reveals how lipase function depends on membrane curvature. *Langmuir* **36**, 6473–6481.

85. Li, L., Hu, J.L., Li, L., Song, F., (2019). Binding constant of membrane-anchored receptors and ligands that induce membrane curvatures. *Soft Matter* **15**, 3507–3514.

86. Goulian, M., Bruinsma, R., Pincus, P., (1993). Long-range forces in heterogeneous fluid membranes. *Europhys Lett* **22**, 145–150.

87. Bruinsma, R., Pincus, P., (1996). Protein aggregation in membranes. *Curr Opin Solid State Mat Sci* **1**, 401–406.

88. Park, J.M., Lubensky, T.C., (1996). Interactions between membrane inclusions on fluctuating membranes. *J Phys I* **6**, 1217–1235.

89. Weikl, T.R., Kozlov, M.M., Helfrich, W., (1998). Interaction of conical membrane inclusions: Effect of lateral tension. *Phys Rev E* **57**, 6988–6995.

90. Mockl, L., (2020). The emerging role of the mammalian glycocalyx in functional membrane organization and immune system regulation. *Front Cell Dev Biol* **8**, 253.

91. Uchimido, R., Schmidt, E.P., Shapiro, N.I., (2019). The glycocalyx: a novel diagnostic and therapeutic target in sepsis. *Crit Care* **23**, 12.

92. Weinbaum, S., Tarbell, J.M., Damiano, E.R., (2007). The structure and function of the endothelial glycocalyx layer. *Annu Rev Biomed Eng* **9**, 121–167.

93. Kuo, J.C.H., Gandhi, J.G., Zia, R.N., Paszek, M.J., (2018). Physical biology of the cancer cell glycocalyx. *Nat Phys* **14**, 658–669.

94. Kanyo, N., Kovacs, K.D., Saftics, A., Szekacs, I., Peter, B., Santa-Maria, A.R., (2020). Glycocalyx regulates the strength and kinetics of cancer cell adhesion revealed by biophysical models based on high resolution label-free optical data. *Sci Rep* **10**, 22422.

95. Hollingsworth, M.A., Swanson, B.J., (2004). Mucins in cancer: Protection and control of the cell surface. *Nat Rev Cancer* **4**, 45–60.

96. Buffone, A., Weaver, V.M., (2020). Don't sugarcoat it: How glycocalyx composition influences cancer progression. *J Cell Biol* **219**, e201910070.

97. Butler, P.J., Bhatnagar, A., (2019). Mechanobiology of the abluminal glycocalyx. *Biorheology* **56**, 101–112.

98. McGuckin, M.A., Linden, S.K., Sutton, P., Florin, T.H., (2011). Mucin dynamics and enteric pathogens. *Nat Rev Microbiol* **9**, 265–278.

99. Mockl, L., Hirn, S., Torrano, A.A., Uhl, B., Brauchle, C., Krombach, F., (2017). The glycocalyx regulates the uptake of nanoparticles by human endothelial cells in vitro. *Nanomedicine* **12**, 207–217.

100. Marshall, B.T., Long, M., Piper, J.W., Yago, T., McEver, R.P., Zhu, C., (2003). Direct observation of catch bonds involving cell-adhesion molecules. *Nature* **423**, 190–193.

101. Mulivor, A.W., Lipowsky, H.H., (2002). Role of glycocalyx in leukocyte-endothelial cell adhesion. *Am. J. Physiol.-Heart Circul. Physiol* **283**, H1282–H1291.

102. Lorz, B.G., Smith, A.S., Gege, C., Sackmann, E., (2007). Adhesion of giant vesicles mediated by weak binding of Sialyl-Lewis^x to E-selectin in the presence of repelling poly(ethylene glycol) molecules. *Langmuir* **23**, 12293–12300.

103. Tarbell, J.M., Pahakis, M.Y., (2006). Mechanotransduction and the glycocalyx. *J Intern Med* **259**, 339–350.

104. Schnitzer, J.E., (1988). Glycocalyx electrostatic potential profile analysis - ion, pH, steric, and charge effects. *Yale J Biol Med* **61**, 427–446.

105. Anderson, M., Moshnikova, A., Engelman, D.M., Reshetnyak, Y.K., Andreev, O.A., (2016). Probe for the measurement of cell surface pH in vivo and ex vivo. *Proc Natl Acad Sci U S A* **113**, 8177–8181.

106. Kharitidi, D., Apaja, P.M., Manteghi, S., Suzuki, K., Malitskaya, E., Roldan, A., (2015). Interplay of endosomal pH and ligand occupancy in integrin $\alpha5\beta1$ ubiquitination, endocytic sorting, and cell migration. *Cell Rep* **13**, 599–609.

107. Arac, D., Boucard, A.A., Ozkan, E., Strop, P., Newell, E., Sudhof, T.C., (2007). Structures of neuroligin-1 and the neuroligin-l/neurexin-1α complex reveal specific protein-protein and protein-Ca^{2+} interactions. *Neuron* **56**, 992–1003.

108. Lipowsky, R., (1995). Bending of membranes by anchored polymers. *Europhys Lett* **30**, 197–202.

109. Shurer, C.R., Kuo, J.C.H., Roberts, L.M., Gandhi, J.G., Colville, M.J., Enoki, T.A., (2019). Physical principles of membrane shape regulation by the glycocalyx. *Cell* **177**, 1757–1770.

110. Hiergeist, C., Lipowsky, R., (1996). Elastic properties of polymer-decorated membranes. *J Phys II* **6**, 1465–1481.

111. Kuznetsova, I.M., Zaslavsky, B.Y., Breydo, L., Turoverov, K.K., Uversky, V.N., (2015). Beyond the excluded volume effects: mechanistic complexity of the crowded milieu. *Molecules* **20**, 1377–1409.

112. Zimmerman, S.B., Trach, S.O., (1991). Estimation of macromolecule concentrations and excluded volume effects for the cytoplasm of Escherichia-coli. *J Mol Biol* **222**, 599–620.

113. Schamel, W.W.A., Alarcon, B., (2013). Organization of the resting TCR in nanoscale oligomers. *Immunol Rev* **251**, 13–20.

114. Vu, V., Light, T., Sullivan, B., Greiner, D., Hristova, K., Leckband, D., (2021). P120 catenin potentiates constitutive E-cadherin dimerization at the plasma membrane and regulates trans binding. *Curr Biol* **31**, 3017–3027.

115. Zhang, Y., Jiang, N., Zarnitsyna, V.I., Klopocki, A.G., McEver, R.P., Zhu, C., (2013). P-selectin glycoprotein ligand-1 forms dimeric interactions with E-selectin but monomeric interactions with L-selectin on cell surfaces. *PLoS One* **8**, e57202.

116. Ramachandran, V., Yago, T., Epperson, T.K., Kobzdej, M.M.A., Nollert, M.U., Cummings, R.D., (2001). Dimerization of a selectin and its ligand stabilizes cell rolling and enhances tether strength in shear flow. *Proc Natl Acad Sci U S A* **98**, 10166–10171.

117. Mockl, L., Pedram, K., Roy, A.R., Krishnan, V., Gustavsson, A.K., Dorigo, O., (2019). Quantitative super-resolution microscopy of the mammalian glycocalyx. *Dev Cell* **50**, 57–72.

118. Johnson, C.P., Fujimoto, I., Rutishauser, U., Leckband, D.E., (2005). Direct evidence that neural cell adhesion molecule (NCAM) polysialylation increases intermembrane repulsion and abrogates adhesion. *J Biol Chem* **280**, 137–145.

119. Shurer, C.R., Colville, M.J., Gupta, V.K., Head, S.E., Kai, F., Lakins, J.N., (2018). Genetically encoded toolbox for glycocalyx engineering: tunable control of cell adhesion, survival, and cancer cell behaviors. *ACS Biomater Sci Eng* **4**, 388–399.

120. Paszek, M.J., DuFort, C.C., Rossier, O., Bainer, R., Mouw, J.K., Godula, K., (2014). The cancer glycocalyx mechanically primes integrin-mediated growth and survival. *Nature* **511**, 319–325.

121. Paszek, M.J., Boettiger, D., Weaver, V.M., Hammer, D.A., (2009). Integrin clustering is driven by mechanical

resistance from the glycocalyx and the substrate. *PLoS Comput Biol* **5**, e1000604.

122. Weikl, T.R., Lipowsky, R., (2004). Pattern formation during T-cell adhesion. *Biophys J* **87**, 3665–3678.

123. Schmid, E.M., Bakalar, M.H., Choudhuri, K., Weichsel, J., Ann, H.S., Geissler, P.L., (2016). Size-dependent protein segregation at membrane interfaces. *Nat Phys* **12**, 704–711.

124. Bell, G.I., (1978). Models for specific adhesion of cells to cells. *Science* **200**, 618–627.

125. Helms, G., Dasanna, A.K., Schwarz, U.S., Lanzer, M., (2016). Modeling cytoadhesion of Plasmodium falciparum-infected erythrocytes and leukocytes-common principles and distinctive features. *FEBS Lett* **590**, 1955–1971.

126. Dembo, M., Torney, D.C., Saxman, K., Hammer, D., (1988). The reaction-limited kinetics of membrane-to-surface adhesion and detachment. *P Roy Soc B-Biol Sci* **234**, 55–83.

127. Singer, S.J., Nicolson, G.L., (1972). The fluid mosaic model of the structure of cell membranes. *Science* **175**, 720–731.

128. Niemela, P.S., Ollila, S., Hyvonen, M.T., Karttunen, M., Vattulainen, I., (2007). Assessing the nature of lipid raft membranes. *PLoS Comput Biol* **3**, 304–312.

129. Lingwood, D., Simons, K., (2010). Lipid rafts as a membrane-organizing principle. *Science* **327**, 46–50.

130. Sezgin, E., Levental, I., Mayor, S., Eggeling, C., (2017). The mystery of membrane organization: composition, regulation and roles of lipid rafts. *Nat Rev Mol Cell Biol* **18**, 361–374.

131. Levental, I., Levental, K.R., Heberle, F.A., (2020). Lipid Rafts: Controversies resolved, mysteries remain. *Trends Cell Biol* **30**, 341–353.

132. Simons, K., Ikonen, E., (1997). Functional rafts in cell membranes. *Nature* **387**, 569–572.

133. Shao, B.J., Yago, T., Setiadi, H., Wang, Y., Mehta-D'souza, P., Fu, J.X., (2015). O-glycans direct selectin ligands to lipid rafts on leukocytes. *Proc Natl Acad Sci U S A* **112**, 8661–8666.

134. Moll, T., Marshall, J.N.G., Soni, N., Zhang, S., Cooper-Knock, J., Shaw, P.J., (2021). Membrane lipid raft homeostasis is directly linked to neurodegeneration. *Essays Biochem* **65**, 999–1011.

135. Simons, K., Gerl, M.J., (2010). Revitalizing membrane rafts: New tools and insights. *Nat Rev Mol Cell Biol* **11**, 688–699.

136. Li, L., Hu, J.L., Rozycki, B., Song, F., (2020). Intercellular receptor-ligand binding and thermal fluctuations facilitate receptor aggregation in adhering membranes. *Nano Lett* **20**, 722–728.

137. Myeong, J., Park, C.G., Suh, B.C., Hille, B., (2021). Compartmentalization of phosphatidylinositol 4,5-bisphosphate metabolism into plasma membrane liquid-ordered/raft domains. *Proc Natl Acad Sci U S A* **118**, 10.

138. Soloviov, D., Cai, Y.Q., Bolmatov, D., Suvorov, A., Zhernenkov, K., Zav'yalov, D., (2020). Functional lipid pairs as building blocks of phase-separated membranes. *Proc Natl Acad Sci U S A* **117**, 4749–4757.

139. Fan, J., Sammalkorpi, M., Haataja, M., (2010). Formation and regulation of lipid microdomains in cell membranes: Theory, modeling, and speculation. *FEBS Lett* **584**, 1678–1684.

140. Simons, K., Sampaio, J.L., (2011). Membrane organization and lipid rafts. *Cold Spring Harbor Perspect Biol* **3**, a004697

141. Viola, A., Gupta, N., (2007). Tether and trap: regulation of membrane-raft dynamics by actin-binding proteins. *Nat Rev Immunol* **7**, 889–896.

142. Destainville, N., (2008). Cluster phases of membrane proteins. *Phys Rev E* **77**, 011905

143. Douglass, A.D., Vale, R.D., (2005). Single-molecule microscopy reveals plasma membrane microdomains created by protein-protein networks that exclude or trap signaling molecules in T cells. *Cell* **121**, 937–950.

144. Li, L., Xu, G.K., Song, F., (2017). Impact of lipid rafts on the T-cell-receptor and peptide-major-histocompatibility-complex interactions under different measurement conditions. *Phys Rev E* **95**, 012403

145. Pralle, A., Keller, P., Florin, E.L., Simons, K., Horber, J.K.H., (2000). Sphingolipid-cholesterol rafts diffuse as small entities in the plasma membrane of mammalian cells. *J Cell Biol* **148**, 997–1007.

146. Pierce, S.K., (2002). Lipid rafts and B-cell activation. *Nat Rev Immunol* **2**, 96–105.

147. Lorent, J.H., Diaz-Rohrer, B., Lin, X.B., Spring, K., Gorfe, A.A., Leventa, K.R., (2017). Structural determinants and functional consequences of protein affinity for membrane rafts. *Nat Commun* **8**, 1219.

148. Simons, K., Ehehalt, R., (2002). Cholesterol, lipid rafts, and disease. *J Clin Invest* **110**, 597–603.

149. Michel, V., Bakovic, M., (2007). Lipid rafts in health and disease. *Biol Cell* **99**, 129–140.

150. Simons, K., Toomre, D., (2000). Lipid rafts and signal transduction. *Nat Rev Mol Cell Biol* **1**, 31–39.

151. Levental, I., Lingwood, D., Grzybek, M., Coskun, U., Simons, K., (2010). Palmitoylation regulates raft affinity for the majority of integral raft proteins. *Proc Natl Acad Sci U S A* **107**, 22050–22054.

152. Murai, T., Sato, C., Sato, M., Nishiyama, H., Suga, M., Mio, K., (2013). Membrane cholesterol modulates the hyaluronan-binding ability of CD44 in T lymphocytes and controls rolling under shear flow. *J Cell Sci* **126**, 3284–3294.

153. Stone, M.B., Shelby, S.A., Nunez, M.F., Wisser, K., Veatch, S.L., (2017). Protein sorting by lipid phase-like domains supports emergent signaling function in B lymphocyte plasma membranes. *Elife* **6**, e19891.

154. Li, L., Hu, J.L., Shi, X.H., Shao, Y.F., Song, F., (2017). Lipid rafts enhance the binding constant of membrane-anchored receptors and ligands. *Soft Matter* **13**, 4294–4304.

155. Mollinedo, F., Gajate, C., (2015). Lipid rafts as major platforms for signaling regulation in cancer. *Adv Biol Regul* **57**, 130–146.

156. Anderson, H.A., Hiltbold, E.M., Roche, P.A., (2000). Concentration of MHC class II molecules in lipid rafts facilitates antigen presentation. *Nat Immunol* **1**, 156–162.

157. Anderson, H.A., Roche, P.A., (2015). MHC class II association with lipid rafts on the antigen presenting cell surface. *Biochim Biophys Acta-Mol Cell Res* **1853**, 775–780.

158. Zhao, J., Wu, J., Veatch, S.L., (2013). Adhesion stabilizes robust lipid heterogeneity in supercritical membranes at physiological temperature. *Biophys J* **104**, 825–834.

159. Li, L., Wang, X.H., Wu, H.L., Shao, Y.F., Wu, H.P., Song, F., (2021). Interplay between receptor-ligand binding and

lipid domain formation depends on the mobility of ligands in cell-substrate adhesion. *Front Mol Biosci* **8**, 655662

160. Li, L., Hu, J.L., Shi, X.H., Rozycki, B., Song, F., (2021). Interplay between cooperativity of intercellular receptor-ligand binding and coalescence of nanoscale lipid clusters in adhering membranes. *Soft Matter* **17**, 1912–1920.

161. Li, L., Hu, J.L., Xu, G.K., Song, F., (2018). Binding constant of cell adhesion receptors and substrate-immobilized ligands depends on the distribution of ligands. *Phys Rev E* **97**, 012405

162. Xiao, H., Woods, E.C., Vukojicic, P., Bertozzi, C.R., (2016). Precision glycocalyx editing as a strategy for cancer immunotherapy. *Proc Natl Acad Sci U S A* **113**, 10304–10309.

163. Mitchell, M.J., King, M.R., (2014). Physical Biology in Cancer. 3. The role of cell glycocalyx in vascular transport of circulating tumor cells. *Am J Physiol-Cell Physiol* **306**, C89–C97.

164. Milusev, A., Rieben, R., Sorvillo, N., (2022). The endothelial glycocalyx: A possible therapeutic target in cardiovascular disorders. *Front Cardiovasc Med* **9**, 897087

165. Murai, T., (2015). Lipid raft-mediated regulation of hyaluronan-CD44 interactions in inflammation and cancer. *Front Immunol* **6**, 420.

166. Yang, Z.S., Qin, W.H., Chen, Y., Yuan, B., Song, X.L., Wang, B.B., (2018). Cholesterol inhibits hepatocellular carcinoma invasion and metastasis by promoting CD44 localization in lipid rafts. *Cancer Lett* **429**, 66–77.

167. Sorice, M., Misasi, R., Riitano, G., Manganelli, V., Martellucci, S., Longo, A., (2021). Targeting lipid rafts as a strategy against coronavirus. *Front Cell Dev Biol* **8**, 618296

168. Washbourne, P., Dityatev, A., Scheiffele, P., Biederer, T., Weiner, J.A., Christopherson, K.S., (2004). Cell adhesion molecules in synapse formation. *J Neurosci* **24**, 9244–9249.

169. Sytnyk, V., Leshchyns'ka, I., Schachner, M., (2017). Neural cell adhesion molecules of the immunoglobulin superfamily regulate synapse formation, maintenance, and function. *Trends Neurosci* **40**, 295–308.

170. Bian, W.J., Miao, W.Y., He, S.J., Qiu, Z., Yu, X., (2015). Coordinated spine pruning and maturation mediated by inter-spine competition for cadherin/catenin complexes. *Cell* **162**, 808–822.

171. Chubykin, A.A., Atasoy, D., Etherton, M.R., Brose, N., Kavalali, E.T., Gibson, J.R., (2007). Activity-dependent validation of excitatory versus inhibitory synapses by neuroligin-1 versus neuroligin-2. *Neuron* **54**, 919–931.

172. Flavell, S.W., Greenberg, M.E., (2008). Signaling mechanisms linking neuronal activity to gene expression and plasticity of the nervous system. *Annu Rev Neurosci* **31**, 563–590.

173. Sudhof, T.C., (2018). Towards an understanding of synapse formation. *Neuron* **100**, 276–293.

174. Miao, Y.L., McCammon, J.A., (2016). G-protein coupled receptors: advances in simulation and drug discovery. *Curr Opin Struct Biol* **41**, 83–89.

175. Mahaut-Smith, M.P., Martinez-Pinna, J., Gurung, I.S., (2008). A role for membrane potential in regulating GPCRs? *Trends Pharmacol. Sci* **29**, 421–429.

176. Vickery, O.N., Machtens, J.P., Zachariae, U., (2016). Membrane potentials regulating GPCRs: insights from experiments and molecular dynamics simulations. *Curr Opin Pharmacol* **30**, 44–50.

177. Vizurraga, A., Adhikari, R., Yeung, J.N., Yu, M.Y., Tall, G. G., (2020). Mechanisms of adhesion G protein-coupled receptor activation. *J Biol Chem* **295**, 14065–14083.